

Where is the black disc limit?

P. Desgrolard¹, L. Jenkovszky², B. Struminsky²

¹ Institut de Physique Nucléaire de Lyon, IN2P3-CNRS et Université Claude Bernard, 43 boulevard du 11 novembre 1918, 69622 Villeurbanne Cedex, France (e-mail: desgrolard@ipnl.in2p3.fr)

² Bogolyubov Institute for Theoretical Physics, National Academy of Sciences of Ukraine, 252143 Kiev, Ukraine (e-mail: jenk,eppaitp@bitp.kiev.ua)

Received: 8 May 1999 / Published online: 22 October 1999

Abstract. By using realistic models for elastic hadron scattering, we demonstrate that at present accelerator energies the s -channel unitarity bound is safe, not to be reached before 10^5 GeV, while the black disc limit is saturated around 6 TeV. By increasing the energy, a larger transparency of the scattered particles near the center, surrounded by a black ring, is expected. Unitarity effects are incorporated and their effects are studied both in a phenomenological and formal, analytical way.

1 Introduction

Our decision to write this paper was motivated partly by recent claims that in high-energy hadron scattering the black disc limit has been reached and the violation of the s -channel unitarity in some models is just around the corner. While the first statement is true and has interesting physical consequences, the second one is wrong for any realistic model fitting the existing data on proton and antiproton scattering up to the highest accelerator energies.

To start with, let us recall the general definitions and notations. Unitarity in the impact parameter (b) representation reads

$$\Im h(s, b) = |h(s, b)|^2 + G_{in}(s, b), \quad (1)$$

where $h(s, b)$ is the elastic scattering amplitude at \sqrt{s} center of mass energy (with $\Im h(s, b)$ usually called the profile function, representing the hadron opacity) and $G_{in}(s, b)$, called the inelastic overlap function, is the sum over all inelastic channel contributions. Integrated over b , (1) reduces to a simple relation between the total, elastic and inelastic cross sections $\sigma_{tot}(s) = \sigma_{el}(s) + \sigma_{in}(s)$.

Equation (1) imposes an absolute limit

$$0 \leq |h(s, b)|^2 \leq \Im h(s, b) \leq 1, \quad (2)$$

while the so-called “black disc” limit $\sigma_{el}(s) = \sigma_{in}(s) = \frac{1}{2}\sigma_{tot}(s)$ or

$$\Im h(s, b) = 1/2 \quad (3)$$

is a particular realization of the optical model, namely it corresponds to the maximal absorption within the eikonal unitarization, when the scattering amplitude is approximated as

$$h(s, b) = \frac{i}{2}(1 - \exp[i\omega(s, b)]), \quad (4)$$

with a purely imaginary eikonal $\omega(s, b) = i\Omega(s, b)$.

Eikonal unitarization corresponds to a particular solution of the unitarity equation

$$h(s, b) = \frac{1}{2} \left[1 \pm \sqrt{1 - 4G_{in}(s, b)} \right], \quad (5)$$

the one with minus sign.

The alternative solution, that with plus sign is known [1, 2] and realized within the so-called U -matrix¹ approach [3, 4] where the unitarized amplitude is

$$h(s, b) = \frac{U(s, b)}{1 - i U(s, b)}, \quad (6)$$

where now U is the input Born term, the analogue of the eikonal ω in (4).

In the U -matrix approach, the scattering amplitude $h(s, b)$ may exceed the black disc limit as the energy increases. The transition from a (central) “black disc” to a (peripheral) “black ring”, surrounding a gray disc, for the inelastic overlap function in the impact parameter space corresponds to the transition from shadowing to antishadowing [1]. We shall present a particular realization of this regime.

The impact parameter amplitude may be calculated either directly from the data, as it was done e.g. in [5, 6] (where, however, the real part of the amplitude was neglected) or by using a particular model that fits the data sufficiently well. There are several models appropriate for this purpose. In the classical paper [7] on this subject, from the behavior of $G_{in}(s, b)$, the proton is characterized as getting “BEL” (Blacker, Edgier and Larger). Below we

¹ We follow traditional terminology, although the word “matrix” in this context is misleading, since U , similar to the eikonal, is a single function rather than a matrix

show that the proton, after having reached its maximal darkness around 6 TeV, may get less opaque beyond.

Actually, the construction of any scattering amplitude rests on two premises: the choice of the input, or Born term and the relevant unitarization procedure (eikonal or U -matrix in our case). Within the present accelerator energy region there are several models that fit the data reasonably well. Compatible within the region of the present experiments, they differ significantly when extrapolated to higher energies. We shall consider two representative examples, namely the Donnachie-Landshoff (D-L) model [8,9] and the dipole Pomeron (DP) model [4,10]

In Sect. 2 we present the necessary details about the two realistic models (D-L and DP), then, focusing on the DP model, we investigate in Sect. 3 the unitarity properties at the Born level and in Sect. 4 we study the optical properties (transparency) after unitarization; a comparison with the D-L model is given in the Appendix.

2 The Born term

The Donnachie-Landshoff (D-L) model [8] is popular for its simplicity. Essentially, it means the following four-parameter empirical fit to all total hadronic cross sections

$$\sigma_{tot} = X s^\delta + Y s^{\delta_r}, \quad (7)$$

where two of the parameters, namely δ (≈ 0.08) and δ_r (< 0) are universal. While the violation of the Froissart-Martin (F-M) bound,

$$\sigma_{tot}(s) < C (\ln s)^2 \quad C = 60 \text{ mb} \quad (8)$$

inherent in that model, is rather an aesthetic than a practical defect (because of the remoteness of the energy where eventually it will overshoot the F-M limit), other deficiencies of the D-L model (or any other model based on a supercritical Pomeron) are sometimes criticized in the literature, but so far nobody was able to suggest anything significantly better instead. A particular attractive feature of the D-L Pomeron, made of a single term, is its factorizability, although this may be too crude an approximation to reality.

The t dependence in the Donnachie-Landshoff model is usually chosen [9] in the form close to the dipole formfactor. For the present purposes a simple exponential residue in the Pomeron amplitude will do as well, with the signature included

$$A(s, t) = -N \left(-i \frac{s}{s_{dl}} \right)^{\alpha(t)} e^{Bt}, \quad (9)$$

where $\alpha(t) = \alpha(0) + \alpha' t$ is the Pomeron trajectory and N is a dimensionless normalization factor related to the total cross section at $s = s_{dl}$ by the optical theorem

$$N = \frac{s_{dl}}{4\pi \sin \frac{\pi}{2} \alpha(0)} \sigma_{tot}(s = s_{dl}). \quad (10)$$

According to the original fits [8,9]: $s_{dl} = 1 \text{ GeV}^2$, $\alpha(0) = 1.08$, $\alpha' = 0.25 \text{ GeV}^{-2}$, and $X = 21.70 \text{ mb}$ (see (7)) resulting in $N = \frac{X}{4\pi \sin \frac{\pi}{2} \alpha(0)} = 4.44$. By identifying

$$\frac{d\sigma(s, t)}{dt} = \frac{d\sigma(s, t=0)}{dt} e^{B_{exp}(s) t} \quad (11)$$

and choosing the CDF or E410 result for the slope B_{exp} at the Tevatron energy, we obtain $B = \frac{1}{2} B_{exp}(s) - \alpha' \ln \frac{s}{s_{dl}} = 4.75 \text{ GeV}^{-2}$.

In the dipole Pomeron (DP) model [4], factorizable at asymptotically high energies, logarithmically rising cross sections are produced at a unit Pomeron intercept alone and thus DP does not conflict with the F-M bound. While data on total cross section are compatible with a logarithmic rise (DP with unit intercept) the ratio σ_{el}/σ_{tot} is found (see [11] for details) for $\delta = 0$ to be a monotonically decreasing function of the energy for any physical value of the parameters. The experimentally observed rise of this ratio can be achieved only for $\delta > 0$ and thus it requires the introduction of a ‘‘supercritical’’ Pomeron, $\alpha(0) > 1$. As a result, the rise of the total cross sections is driven and shared by the dipole and the ‘‘supercritical’’ intercept. The parameter $\delta = \alpha(0) - 1$ in the DP model is nearly half that of the D-L model, making it safer from the point of view of the unitarity bounds. Generally speaking, the closer the input to the unitarized output, the better the convergence of the unitarization procedure.

Let us remind that, apart from the conservative F-M bound, any model should satisfy also s -channel unitarity. We demonstrate below that both the D-L and DP model are well below this limit and will remain so within the foreseeable future. (Let us remind that the D-L and the DP model are close numerically, although they are different conceptually and consequently they extrapolations to superhigh energies will differ as well.)

The elastic scattering amplitude corresponding to the exchange of a dipole Pomeron reads

$$A(s, t) = \frac{d}{d\alpha} \left[e^{-i\pi\alpha/2} G(\alpha) (s/s_0)^\alpha \right] \\ = e^{-i\pi\alpha/2} (s/s_0)^\alpha \left[G'(\alpha) + (L - i\pi/2) G(\alpha) \right], \quad (12)$$

where $L \equiv \ln \frac{s}{s_0}$, $\alpha \equiv \alpha(t)$ is the Pomeron trajectory; in this paper, for simplicity we use a linear trajectory $\alpha(t) = \alpha(0) + \alpha' t$.

By identifying $G'(\alpha) = -a e^{b_p(\alpha-1)}$, (12) can be rewritten in the following geometrical form

$$A(s, t) = i \frac{as}{b_p s_0} \left[r_1^2(s) e^{r_1^2(s)[\alpha(t)-1]} \right. \\ \left. - \epsilon r_2^2(s) e^{r_2^2(s)[\alpha(t)-1]} \right], \quad (13)$$

where

$$r_1^2(s) = b_p + L - i \frac{\pi}{2}; \quad r_2^2(s) = L - i \frac{\pi}{2}. \quad (14)$$

The model contains the following adjustable parameters: a , b_p , $\alpha(0)$, α' , ϵ and s_0 .

Table 1. Parameters of the dipole Pomeron found in [10], where the Odderon and two secondary Reggeons ω and f were also included

a	b_p	$\alpha(0)$	$\alpha'(\text{GeV}^{-2})$	ϵ	$s_0(\text{GeV}^2)$
355.6	10.76	1.0356	0.377	0.0109	100.0

In Table 1 we quote the numerical values of the parameters of the dipole Pomeron fitted in [10] to the data on proton-proton and proton-antiproton elastic scattering:

$$\sigma_{tot}(s) = \frac{4\pi}{s} \Im m A(s, 0), \quad \rho(s) = \frac{\Re A(s, 0)}{\Im m A(s, 0)} ;$$

$$4 \leq \sqrt{s}(\text{GeV}) \leq 1800 \quad (15)$$

as well as the differential cross section

$$\frac{d\sigma(s, t)}{dt} = \frac{\pi}{s^2} |A(s, t)|^2 ; \quad 23.5 \leq \sqrt{s}(\text{GeV}) \leq 630 ;$$

$$0 \leq |t|(\text{GeV}^2) \leq 6 . \quad (16)$$

In that fit [10], apart from the Pomeron, the Odderon and two subleading trajectories ω and f were also included. Here, for simplicity and clarity we consider only the dominant term at high energy due to the Pomeron exchange with the parameters fitted in [10]. The extent to which this Pomeron is a good approximation in the TeV region is discussed in details in [12]. The quality of this fit is illustrated and discussed in [10]. With such a simple model and small number of parameters, better fits are hardly to be expected.

We use the above set of parameters to calculate the impact parameter amplitude, and to scrutinize in Sect. 3 the unitarity properties of this Born level amplitude. In Sect. 4 we introduce a unitarization procedure, necessary at higher energies and discuss the relevant physical consequences.

To summarize, the DP model with a unit intercept is selfconsistent in the sense that its functional (logarithmic) form is stable with respect to unitarization. Moreover, the presence of the second term, proportional to ϵ in (13) has the meaning of absorptions and it is essential for the dip mechanism. It can be viewed also as one more unitarity feature of the model.

In the limit of very high energies, when $L \gg b_p$ the two (squared) radii $R_i^2 = \alpha' r_i^2$ become equal and real and the model obeys exact geometrical scaling as well as factorization (see next section). Alternatively, it corresponds to the case of no absorptions ($\epsilon = 0$).

However attractive, the case of a unit intercept ($\delta = 0$) is only an approximation to the more realistic model, requiring $\delta > 0$ to meet the observed rise of the ratio σ_{el}/σ_{tot} . For such a ‘‘supercritical’’ Pomeron unitarization becomes inevitable.

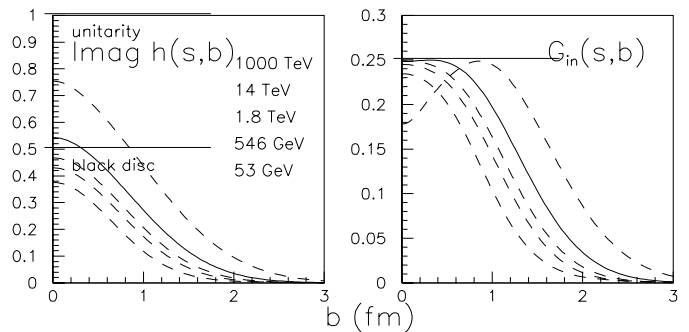


Fig. 1. Calculated Born level $\Im m h(s, b)$ and $G_{in}(s, b)$ plotted versus the modulus of the impact parameter b for some characteristic energies \sqrt{s} as indicated (the highest and largest plots are for the largest energy, the solid curve is for the LHC energy). The top of the scale on the left is the unitarity limit and the value 1/2 corresponds to the black disc limit. The calculations are performed for the dipole Pomeron model of [10]; similar results are obtained for the D-L model (see the text)

3 Impact parameter representation, the black disc limit and unitarity

The elastic amplitude in the impact parameter representation in our normalization is at the Born level

$$h(s, b) = \frac{1}{2s} \int_0^\infty dq q J_0(bq) A(s, -q^2), \quad q = \sqrt{-t}. \quad (17)$$

The impact parameter representation for linear trajectories² is calculable explicitly for the DP model (13)

$$h(s, b) = i g_0 [e^{r_1^2 \delta} e^{-b^2/4R_1^2} - \epsilon e^{r_2^2 \delta} e^{-b^2/4R_2^2}], \quad (18)$$

where

$$R_i^2 = \alpha' r_i^2 \quad (i = 1, 2) \quad ; \quad g_0 = \frac{a}{4b_p \alpha' s_0}. \quad (19)$$

Asymptotically (*i.e.* when $L \gg b_p$, *i.e.* $\sqrt{s} \gg 2$ TeV, with the parameters of Table 1),

$$h(s, b) \xrightarrow{s \rightarrow \infty} i g(s) (1 - \epsilon) e^{-\frac{b^2}{4R^2}}, \quad (20)$$

where

$$R^2 = \alpha' L \quad ; \quad g(s) = g_0 \left(\frac{s}{s_0} \right)^\delta. \quad (21)$$

To illustrate the s -channel unitarity, we display in Fig. 1 a family of curves showing the imaginary part of the amplitude in the impact parameter-representation at various energies; also shown is the calculated (from (1)) inelastic overlap function.

Our confidence in the extrapolation of $\Im m h(s, b)$ to the highest energies rests partly on the good agreement of our (non fitted) results with the experimental analysis of the central opacity of the nucleon (see Table 2).

² Other cases were treated *e.g.* in [4]

Table 2. Central opacity of the nucleon $\Im m h(s, 0)$ calculated with the model [10] at ISR, SPS, Tevatron energies compared with experiment

\sqrt{s}	53 GeV	546 GeV	1800 GeV
exp	0.36 [6]	0.420 ± 0.004 [13]	0.492 ± 0.008 [14]
th	0.36	0.424	0.461

It is important to note that the unitarity bound 1 for $\Im m h(s, b)$ will not be reached at the LHC energy, while the black disc limit $1/2$ will be slightly exceeded, the central opacity of the nucleon being $\Im m h(s, 0) = 0.54$.

The black disc limit is reached at $\sqrt{s} \sim 6$ TeV, where the overlap function reaches its maximum $\frac{1}{4}$. This energy corresponds to the appearance of the antishadow mode in agreement with the general considerations in [1]. Notice that while $\Im m h(s, b)$ remains central all the way, $G_{in}(s, b)$ is getting more peripheral as the energy increases starting from the Tevatron. For example, at $\sqrt{s} = 14$ TeV, the central region of the antishadowing mode below $b \sim 0.4$ fm is discernible from the peripheral region of shadowing mode beyond $b \sim 0.4$ fm, where $G_{in}(s, b) = \frac{1}{4}$. In terms of [7], the proton will tend to become more transparent (gray) at the center, surrounded by a black ring, *i.e.* it is expected to become “GEL” instead of “BEL”.

The s channel unitarity limit will not be endangered until extremely high energies (10^5 for the D-L model and 10^6 GeV for the DP), which is secure for any credible experiment. It is interesting to compare these limit with the limitations imposed by the Froissart-Martin bound: actually the Pomeron amplitude saturates the F-M bound at 10^{27} GeV. As expected, the F-M bound is even more conservative than that following from s -channel unitarity.

The D-L and DP models are confronted in the Appendix.

4 Unitarization

4.1 Generalities

Now, we consider the unitarized amplitude which, according to the “ U -matrix” prescription [3, 4] and in the impact parameter representation, writes

$$H(s, b) = \frac{h(s, b)}{1 - ih(s, b)}, \quad (22)$$

with the Born term $h(s, b)$ defined in the previous section in (13)-(14).

We study at various energies the behavior of this amplitude $H(s, b)$ and of the corresponding inelastic overlap function

$$\tilde{G}_{in}(s, b) = \Im m H(s, b) - |H(s, b)|^2. \quad (23)$$

By comparing it with the similar results obtained at the Born level, we found that unitarization lowers significantly

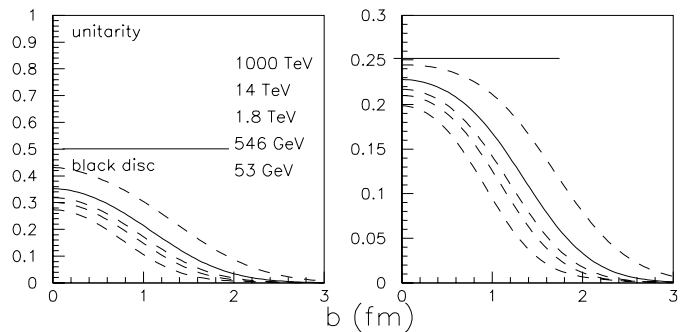


Fig. 2. Same as in Fig. 1, for the unitarized amplitude $H(s, b)$ and the overlap function $\tilde{G}_{in}(s, b)$, calculated without refitting the parameters used in [10] at the Born level

both the elastic and inelastic impact parameter amplitudes, at least if the parameters are kept the same (compare Figs. 1–2).

An unescapable consequence of the unitarization is that, when calculating the observables, one should also replace the Born amplitude $A(s, t)$ by a unitarized amplitude $\tilde{A}(s, t)$ defined as the inverse Fourier-Bessel transform of $H(s, b)$

$$\tilde{A}(s, t) = 2s \int_0^\infty db b J_0(b\sqrt{-t}) H(s, b). \quad (24)$$

Thus, the above picture may change since the parameters of the model should in principle be refitted under the unitarization procedure (this effect of changing the parameters was clearly demonstrated *e.g.* in [15]).

Actually, searching for a new fit of the parameters using an “exact” unitarization procedure is time consuming and unnecessary for the present discussion because the behavior of the amplitude and of the overlap function in the impact parameter representation obtained at the Born level will be almost restored after unitarization. We checked that the parameters of the complete model (with the secondary Reggeons and Odderon added in the fit) after unitarization may be rearranged so as to reproduce well the data and give roughly the same extrapolated properties as at the Born level. While the unitarity limit now is secured automatically (remind that $\Im m h(s, 0)$ is well below that limit even at the Born level in the TeV region) the behavior of the elastic impact parameter amplitude after it has reached the black disc limit corresponds (see [1]) to the transition from shadowing to antishadowing. In other words, the proton (antiproton) after having reached its maximal blackness around 6 TeV, will become progressively more transparent with increasing energies at its center (becoming a gray disc surrounded by a black ring).

4.2 Analytic method of unitarization

Above we presented calculations based on two models: a “selfconsistent” DP ansatz fitted to the data at the Born level and the same model with eikonalization. As

expected, unitarity (eikonalization) modifies (lowers) the impact parameter amplitude significantly. Actually, after the unitarization process, as already stressed, the parameters should be refitted and, as demonstrated in [15] for the total cross sections, they are expected to change quite a lot. Since relevant (*i.e.* with unitarization involved) fits to the differential cross sections are technically complicated, below we present a simple and elegant (analytic) approach to this problem.

Let us write the Born amplitude in the following Pomeron geometrical form (for simplicity, below we neglect the real part), intended for energies $\ln(s/s_0) \gg \pi/2$,

$$h(s, b) \simeq i\tilde{g}(s)e^{-\frac{b^2}{4R^2}}, \quad (25)$$

with

$$R^2 = \alpha' \ln\left(\frac{s}{s_0}\right) \quad ; \quad \tilde{g}(s) = \tilde{g}_0 \left(\frac{s}{s_0}\right)^\delta. \quad (26)$$

This corresponds to a dipole Pomeron, taken alone, with a single exponential in the DP model of the previous sections, but without absorptions, $\epsilon = 0$, now supposed to be generated by unitarity, the “running coupling” $\tilde{g}(s)$ being as before and $\alpha(0) = 1 + \delta$. This approximation to the DP is justified at very high energies, when $\ln(s/s_0) \gg b_p$ and the two radii and exponentials become equal and real; accordingly $\tilde{g}(s)$ is renormalized by absorbing ϵ (see (20-21)). In the U -matrix approach, the unitarized impact parameter amplitude is defined by (22), while the inelastic overlap function is by (23). It is quite easy to evaluate the dynamics of the hadron opacity $\Im m H(s, b)$ and of $\tilde{G}_{in}(s, b)$, *i.e.* their s and b dependence, providing we have estimated the relevant parameters to be used after unitarization.

By accepting this “asymptotic” approximation, we have assumed $\ln(s/s_0) \gg b_p$ and $\pi/2$. The last condition constrains s_0 and b_p as shown in Table 1, in order to give a more acceptable lower energy limit (by increasing the domain of the present approximation). For example, we may choose the traditional “scale” parameter $s_0 = 1 \text{ GeV}^2$. To evaluate the crucial parameter δ , we used the ratio of the cross sections σ_{el}/σ_{tot} , as calculated in [11] in the U -matrix approach with rescattering corrections included up to $\left(1/\ln(s/s_0)\right)$

$$\frac{\sigma_{el}}{\sigma_{tot}} \simeq 1 - \frac{\tilde{g}(s)}{(1 + \tilde{g}(s)) \ln(1 + \tilde{g}(s))}, \quad (27)$$

where $\tilde{g}(s)$ is defined by (26). The only variable $\tilde{g}(s)$ appearing in this equation can be determined from the experimental data on the ratio σ_{el}/σ_{tot} . To minimize the subleading contributions, we choose the two highest energy points at 546 GeV and at 1.8 TeV. By solving (27) numerically we find for each of the experimental values the corresponding values of $\tilde{g}(s)$ (see Table 3).

Note that, when using the same hypothesis as in (25)

$$h(s, b) \simeq ig_B(s)e^{-\frac{b^2}{4R^2}}, \quad (28)$$

Table 3. Values of the function $\tilde{g}(s)$ entering the asymptotic impact parameter amplitude, estimated for the two highest energies from experiments [16] concerning σ_{el}/σ_{tot}

	UA4	CDF	E710	CDF
\sqrt{s} (GeV)	546	546	1800	1800
σ_{el}/σ_{tot}	$.215 \pm .005$	$.210 \pm .002$	$.230 \pm .012$	$.246 \pm .004$
$\tilde{g}(s)$	$.658 \pm 0.023$	$.635 \pm .009$	$.730 \pm .060$	$.811 \pm .021$

Table 4. Parameters of the approximate Born Dipole Pomeron amplitude in the b representation yielding an analytical treatment of the unitarization

\tilde{g}_0	$\alpha(0)$	$\alpha'(\text{GeV}^{-2})$	$s_0(\text{GeV}^2)$
0.175	1.102	0.25	1.0

we find at the Born level, instead of (27),

$$\left(\frac{\sigma_{el}}{\sigma_{tot}}\right)_{Born} \simeq \frac{\Im m h(s, 0)}{2} = \frac{g_B(s)}{2}. \quad (29)$$

This means that the Born coupling $g_B(s)$ is renormalized (increased) by the unitarization process since it is clear from Table 3 that $\tilde{g}(s) > g_B(s)$.

By using the ratio of two \tilde{g} 's, taken at two different energies

$$\frac{\tilde{g}(s_2)}{\tilde{g}(s_1)} = \left(\frac{s_2}{s_1}\right)^\delta$$

the parameter δ can be determined from $\delta = \ln(g(s_2)/g(s_1))/\ln(s_2/s_1)$ at least in theory. By using the experimental values of $\tilde{g}(s)$ quoted above we find a large discrepancy due the large errors. If we rely on the most precise data (CDF [13,14]) we find $\delta = 0.102 \pm 0.040$, seemingly high, compared with our Born value. However such a crude estimate (even when choosing the central value) is in a surprisingly good agreement with most recent determinations of the Pomeron intercept and exhibits the increase due to the unitarization process investigated in [15]. Notice that the less precise pair of data (UA4, E710) does not allow to determine δ with a credible precision: $\delta = 0.043 \pm 0.120$ with that pair of data and 0.058, 0.087 when choosing the other possibilities. By choosing $s_0 = 1 \text{ GeV}^2$ for the reason explained above, and for $\delta = 0.102$, the definition of $\tilde{g}(s)$ gives a norm $\tilde{g}_0 = 0.174 \pm 0.002$ for both the CDF values obtained at 546 and 1800 GeV (again, for consistency we do not take into account the less precise determinations of $g(s)$). The remaining parameter α' necessary in the evaluation of the radius R will be chosen for simplicity equal to its world average value 0.25 GeV^2 . These parameters are collected in Table 4.

With these numbers in hand, it is now straightforward to calculate $\Im m H(s, b)$ and $\tilde{G}_{in}(s, b)$. The results are shown in Fig. 3.

They appear to be similar to those exhibited in Fig. 1 except for the lowest energies (say at ISR, where our high-energy approximation is not valid any more). Thus, as far as the TeV region is concerned, the modifications of Fig. 1

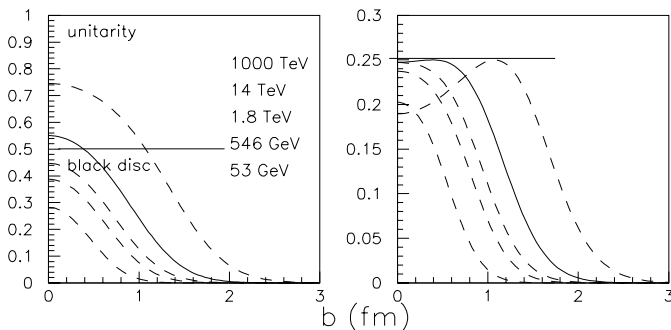


Fig. 3. Same as in Figs. 1–2, for the unitarized amplitude $H(s, b)$ and the overlap function $\widetilde{G}_{in}(s, b)$, calculated in the simple asymptotic analytical approximation of the Pomeron, with a specific determination of the parameters

are in practice negligible, when using the above simplified unitarization. It confirms our statement above, that little changes with respect to the Born level are to be expected after unitarization, provided if the original parameters are refitted. The above approximate analytic unitarization with the “integral” fit to the ratio of the cross sections, is more economic than refitting the parameters by using the whole machinery of exact eikonalization of the full amplitude. Furthermore, it appears that our supercritical DP model at the Born level ((12) or (13)) mimics the situation when rescattering corrections are taken into account, and no problems are expected with the violation of unitarity.

In other words, while in the “self-consistent” DP ansatz absorptions (unitarity) effect, giving rise e.g. to the dip-bump structure are built in right from the beginning, here the Born term is simpler since absorptions are supposed to be generated by unitarization. Although these two models, have some common features, they are not identical (even if we neglect the Odderon and Reggeons). Notice that the (close) black disc- and (remote) unitarity limits both concern the delicate central (near $b = 0$) region where the s -channel unitarity effects are important. Various approaches to s -channel unitarity may clarify the optical and geometrical properties (“transparency”) of the colliding hadrons as well as the efficiency of the existing unitarization procedures.

5 Conclusions

While the results of our analysis in the impact parameter representation are in agreement with the earlier observations that $\Im h(s, b)$ remains central and $G_{in}(s, b)$ becomes peripheral as the energy exceeds several TeV (see Fig. 1). There is a substantial difference with the known “BEL-picture” [7], according to which with increasing energy the proton becomes Blacker, Edgier and Larger.

We confirm that getting edgier and larger, the proton, after reaching its maximal blackness, will tend to be more transparent or “GEL” (a gray disc surrounded by a black ring) when the energy exceeds that of the Tevatron. This

Table 5. Maximum values of the amplitude and overlap function at the Born level and after U -matrix unitarization calculated at 14 TeV for the DP and D-L models without refitting the parameters

	$\Im h(s, 0)$	$G_{in}(s, 0)$	$\Im H(s, 0)$	$\widetilde{G}_{in}(s, 0)$
DP	0.535	0.247	0.349	0.227
D-L	0.539	0.246	0.351	0.227

transition from shadowing to new antishadowing scattering mode is expected to occur at the LHC.

To conclude, we stress once more that both the data and relevant models at present energies are well below the s -channel unitarity limit. In our opinion, deviations due to the diversity of realistic models may result in discrepancies concerning $\Im h(s, 0)$ at the level of at most 10%, while its value at 6 TeV is still half that of the unitarity limit, so there is no reason to worry about it! Therefore, model amplitudes at the Born level may still be quite interesting and efficient in analyzing the data at present accelerator energies and giving some predictions beyond. The question, which model is closer to reality and meets better the requirements of the “fundamental theory” remains of course topical.

Extrapolations and predictions to the energies of the future accelerators (see e.g. [12]) are both useful and exciting since they will be checked in the not-so-far future at LHC and other machines. The fate of the “black disc limit” is one among these.

Acknowledgements. We thank S.M. Troshin for a useful correspondence.

Appendix: comparison between the DP and D-L models

The D-L amplitude in the impact parameter representation at the Born level, calculated from (9) and (17) is

$$h(s, b) = -\frac{N}{2s} \left(-i \frac{s}{s_{dl}} \right)^{\alpha(0)} \frac{e^{-\frac{b^2}{4B'(s)}}}{2B'(s)},$$

$$B'(s) = B + \alpha' \left(\ln \frac{s}{s_{dl}} - i \frac{\pi}{2} \right).$$

As already noted, the s channel unitarity limit both for the DP and the D-L model will not be endangered until extremely high energies (10^5 GeV for the DP and 10^6 GeV for the D-L model, the order-of-magnitude differences coming from the smaller intercept in the DP model), while the F-M bound is saturated at 10^{27} GeV (for more details see [17]).

Table 5 presents a selection of results concerning the DP and D-L models for the Pomeron in the impact parameter representation of the elastic amplitude and inelastic overlap function, calculated at $b = 0$ at the LHC energy.

We conclude that the two models give similar results; all relevant conclusions on unitarity and black disc limits for DP model hold for D-L model as well (the curves in Figs. 1,2 would be indistinguishable by eye).

Note that both models are supercritical, with asymptotic s^δ type behavior of the total cross sections. They are known to give fits which cannot be discriminated by present data from an asymptotic $\ln^2 s$ type behavior. This is another argument to neglect in that case unitarization effects.

References

1. See: S.M. Troshin, N.E. Tyurin, Beyond the black disc limit: from shadowing to antishadowing scattering mode, hep-ph/9810495, and earlier references therein
2. A. Basetto, F. Paccanoni, Nuovo Cim. A **61** (1969) 486
3. V. Savrin, N. Tyurin, O. Khrustalev, El. Chast. i Atom. Yadra (Engl. transl.: Sov. J. Particles and Nuclei) **7** (1976) 21
4. See: A.N. Vall, L.L. Jenkovszky, B.V. Struminsky, Sov. J. Particles and Nuclei **19** (1988) 77, and earlier references therein
5. U. Amaldi, K.R. Schubert, Nucl. Phys. B **166** (1980) 301
6. R. Castaldi, G. Sanguinetti, Ann. Rev. Nucl. Part. Sci. **35** (1985) 351
7. R. Henzi, P. Valin, Phys. Lett. B **132** (1983) 443
8. A. Donnachie, P.V. Landshoff, Phys. Lett. B **296** (1992) 227
9. A. Donnachie, P.V. Landshoff, Z. Phys. C **2** (1979) 55; Phys. Lett. B **123** (1983) 345; Nucl. Phys. B **231** (1983) 189; *ibid* **244** (1984) 322
10. P. Desgrolard, M.Giffon, L. Jenkovszky, Z. Phys. C **55** (1992) 637
11. L.L. Jenkovszky, B.V. Struminsky, A.N. Vall, Yad. Fizika (Engl. transl.: Sov. J. Nucl. Phys.) **46** (1987) 1519
12. S. Chatrchian et al., work in progress
13. S. Abe et al., CDF Collaboration, Phys. Rev. D **50** (1994) 550
14. P. Giromini, CDF Collaboration, in Proceedings of International Conference on Elastic and diffractive scattering (5th "Blois workshop"), edited by H.M. Fried, K. Kang, C-I. Tan (World scientific, Singapore, 1993), p.30
15. R.J.M. Covolan, J. Monthanha, K. Goulianos, Phys. Lett. B **389** (1996) 176
16. These data are quoted by G. Matthiae, Rep. Prog. Phys. **57** (1994) 743
17. M. Bertini, P. Desgrolard, Yu. Ilyin, Int. J. Physics, **1** (1995) 45